

**RADAR DETECTIONS OF ICE WITHIN LOBATE FLOWS IN NEREIDUM MONTES, MARS.** Daniel C. Berman, Isaac B. Smith, Frank C. Chuang, and David A. Crown, Planetary Science Institute, 1700 E. Ft. Lowell Rd., Suite 106, Tucson, AZ 85719; [bermandc@psi.edu](mailto:bermandc@psi.edu).

**Introduction:** Recent mapping of ice-rich flow features in the southern mid-latitudes [1-3] coupled with analyses using high resolution images have identified Nereidum Montes, along the northern portion of Argyre basin ( $\sim 35^{\circ}$ - $45^{\circ}$ S,  $\sim 300^{\circ}$ - $330^{\circ}$ E), as the location of the largest concentration of ice-rich flow features in the southern mid-latitudes. Here, mantling deposits and ice-rich landforms cover larger areas of the surface, are better preserved, and show more complete sequences of both degradation and mobilization than in eastern Hellas. For these reasons, studies of Nereidum Montes will yield critical constraints on Mars' recent geological and climate histories.

**Ice-rich flow features in Nereidum Montes:** Lobate debris aprons (LDAs) are masses of material with lobate terminations that typically extend down and sometimes beyond the slopes of high-relief features such as massifs, mesas, canyon walls, and crater walls. Apron planform shapes, surface lineation patterns, and topographic profiles [e.g., 4] suggest viscous flow/deformation of material. Proposed terrestrial analogues include rock glaciers [e.g., 5], debris-covered glaciers [e.g., 6, 7], and wet or icy debris flows [e.g., 8, 9]. Modeled radar sounding data of Deuteronilus Mensae and eastern Hellas indicate massive internal ice within LDAs, rather than ice lenses filling interstitial zones between boulders [10-12]. We have identified numerous LDAs in Nereidum Montes.

Lobate, viscous flow features are observed on slopes (e.g., crater walls and hills) throughout the southern mid-latitudes [e.g., 13-15]. These features are typically bound by moraine-like ridges and their surfaces are commonly pitted, resembling eroded mantling deposits. The size and shape of the lobes are controlled by local topography. They are commonly associated with gullies and arcuate ridges and, unlike LDAs, are thought to be derived from downslope movement of mantling deposits [14, 16, 17]. Many lobate flows in Nereidum Montes retain clear examples of well-preserved ice-rich deposits within their margins, rather than deflated and/or degraded morphologies. Large viscous flow features observed emanating from massifs (Fig. 2) contain surface flow features such as lineations, crevasses, and lobate margins [e.g., 18]. Lobate flow features have been interpreted to be debris covered glaciers or rock glaciers [5, 15, 19, 20]. Lobate flow features in other

regions tend to superpose LDAs and crater counts show them to be younger features [e.g., 15, 21].

**Data and Methods:** Mars Reconnaissance Orbiter (MRO) Shallow Radar (SHARAD) data detect subsurface interfaces such as those between ice and rock at the bottom of lobate flow features [10]. SHARAD records power and time, producing a 2-dimensional cross-sectional profile of surface and subsurface reflections as the spacecraft passes over a target. Reflections from cross track topography (clutter) may arrive at delay times similar to those of subsurface reflectors and need to be mitigated by comparing the observation to a simulated radar image generated from a DEM (Fig. 2b, technique described in detail in [23]). Reflections that occur in both must be excluded from interpretation.

The dielectric value for ice (calculated from laboratory and empirical studies for Earth and Mars) is 3.15 [24, 25], representing a reduction in light speed from that of a vacuum and delays the subsurface reflection. We correct for this by changing the velocity of light below the surface return to match that of ice:  $c/\sqrt{3.15}$ .

**Results:** SHARAD observation 3521801 crosses a lobate flow feature in Fig. 1. Analysis of the radargram reveals a potential basal reflector (Figure 2, white arrows) that does not appear in the MOLA DEM simulation (Fig. 2b), confirming the detection. Correcting for the dielectric value of ice (Fig. 2c) creates a near perfect continuation of the flat plane to the north under the lobate flow feature. Thus, the velocity of electromagnetic waves in this material is consistent with the velocity in water ice.

Ice volumes can be calculated using a combination of SHARAD detections and Digital Terrain Models (DTMs). We have performed a simplified proof of concept test for an LDA in eastern Hellas (Fig. 3, centered at  $40.6^{\circ}$ N,  $103^{\circ}$ E), where LDAs have been studied previously with SHARAD data [10]. Analysis of a series of basal depths from reflectors along SHARAD track 3974301 over the LDA gives a mean depth of 209 m. The individual values were used as a baseline to estimate LDA thickness across part of the apron, in combination with a DTM produced from CTX images D15\_032978\_1391 and F22\_044411\_1391. The area of the LDA was previously mapped as  $1647 \text{ km}^2$  [21]. For the portion covered by the DTM, these values produced a total ice volume of  $\sim 155 \text{ km}^3$ . In future work, this process will be applied to features in

Nereidum Montes to estimate the ice budget for the region.

**References:** [1] Berman, DC et al. (2014), *LPSC 45*, abstract 1553. [2] Chuang, FC et al. (2014a), *LPSC 45*, abstract 2081. [3] Chuang, FC et al. (2014b), *LPSC 45*, abstract 2066. [4] Grindrod, PM and SA Fawcett (2011), *GRL*, 38(19). [5] Whalley, WB and F Azizi (2003), *JGR 108(E4)*, 8032. [6] Baker, DMH et al. (2010), *Icarus 207*, 186-209. [7] Levy, JS et al. (2014), *JGR 119*, 2188-2196. [8] Squyres, SW (1978), *Icarus 24*, 600-613. [9] Baratoux, D et al. (2002), *GRL 29(7)*. [10] Holt, JW et al. (2008), *Science 322*, 1235-1238. [11] Plaut, JJ et al. (2009), *GRL 36*, L02203. [12] Plaut, JJ et al. (2010), *LPSC 41*, abstract 2454. [13] Milliken, RE et al. (2003), *JGR 108*. [14] Berman, DC et al. (2009), *Icarus 200*, 77-95. [15] Hartmann, WK et al. (2014), *Icarus 228*, 96-120. [16] Berman, DC et al. (2005), *Icarus 178*, 465-486. [17] Head, JW et al. (2003), *Nature 426*, 797-802. [18] Hubbard, B et al. (2014), *Cryosphere 8*, 2047-2061. [19] Arfstrom, J and WK Hartmann (2005), *Icarus 174*, 321-335. [20] Sounness, C et al. (2012), *Icarus 217*, 243-255. [21] Berman, DC et al. (2015), *PSS 111*, 83-99. [22] Smith, IB and JW Holt (2010), *Nature 465(7297)*, 450-453. [23] Smith, IB and JW Holt (2015), *JGR*. [24] Gough, SR (1972), *Can J Chem 50*, 3046-3051. [25] Grima, C et al. (2009), *GRL 36*, L03203.

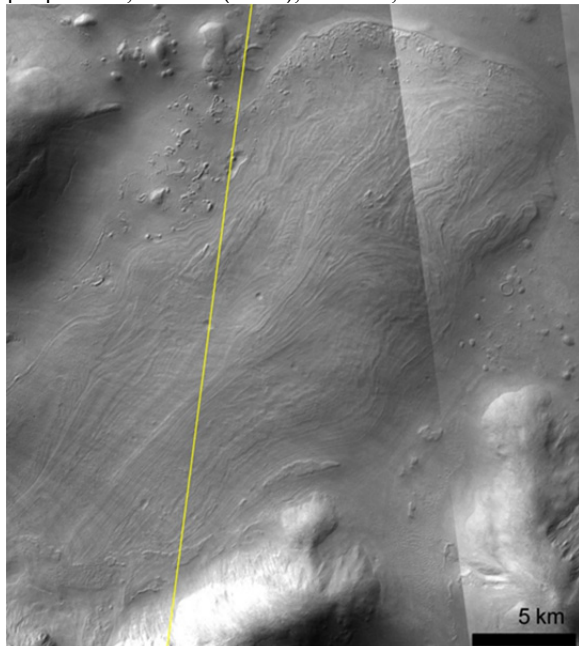


**Figure 1** Lobate flow feature in Nereidum Montes extending to the NE from massif. SHARAD track in yellow (shown in Fig. 2c below). CTX mosaic centered at 47° S, 327°E.

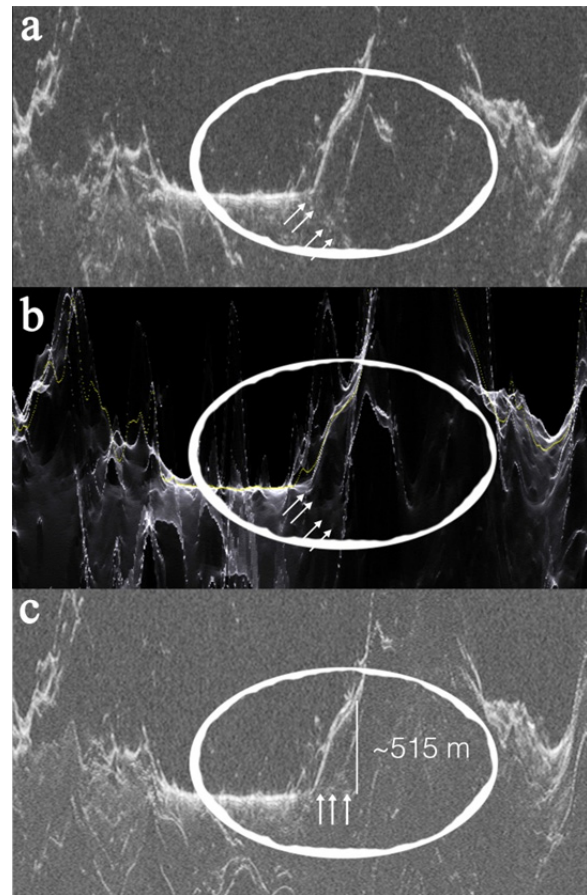


**Figure 2** Comparison of SHARAD observations to synthetic and depth corrected radargrams for the track shown in Fig. 1 in Nereidum Montes; a) SHARAD observation 3521801 with a subsurface reflector (arrows); b) synthetic simulation using MOLA DEM without surface echoes, confirming the subsurface detection; c) depth-corrected version using the velocity of light in ice.

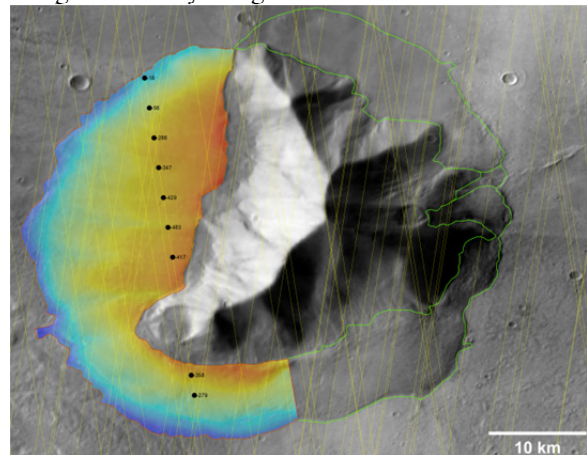


**Figure 3** THEMIS IR daytime mosaic showing LDA in eastern Hellas with CTX DTM superposed in color. SHARAD tracks shown in yellow. Depths to basal reflector shown by black dots.